UTRECHT UNIVERSITY

MASTER THESIS PROJECT

Hair Rendering: Importance Sampling of Dual Scattering Approximation

Author:
Jeffrey LEMEIN

Supervisor:
Prof. Remco VELTKAMP
Dr. Robby T. TAN
Desmond CHIK
Daniel HECKENBERG

September 6, 2019

Abstract

Your abstract goes here... ...

Contents

Chapter 1

Introduction

Hair rendering has always been a challenging task due to the amount of hair strands and the complex scattering behaviour between them. A human head may consist of over 100.000 hair strands and rendering them in a realistic and efficient way is challenging. Furry animals may even consist of over millions of hair strands. It is easy to see that the amount of strands provides us with a big challenge. Efficient rendering models should be devised.

Hair rendering becomes more important as more physically accurate models are constructed. The following number of industries benefit from realistic looking hair models:

- Animation movie industry: to efficiently render realistic hair, instead of simplified models.

- Game industry to enhance realism and for better visual effects.

- Clothes manufacturers: to be able to realistically render custom fabrics and see what the visual appearance of the fiber structure will look like under different lighting conditions.

- Hair styling industry: to realistically render the appearance of hair styling products applied to the hair.

Since rendering individual fibers is very time consuming, a lot of work has been put into approximating the appearance of a hair volume. For example, approximations can be performed by applying transparent textures to a bounding volume to give the illusion of a realistically looking hair model. However this approach might work well for a still image or for applications that do not focus on hair so much, but is not very flexible for movie or game industries. These industries often have dynamic environments in which hair might be animated or lights may change position, leading to shifting highlights that are more difficult to manage using non-physical based approaches.

Nowadays, improved hardware makes it possible to render models of individual fibers. This opens the door to physically based models based on ray-tracing. Path-tracing is the most realistic way of rendering the fibers by considering all the scattering events between light rays and individual fibers and consequently adding up the contributions along the way. It still takes up a substantial amount of time to render a single frame. The time is heavily dependent on the amount of hair fibers, but to overcome the hundred of thousands of hair strands, efficient rendering models should be devised.

1.1   Goal and approach

In this thesis project the goal is to extend the dual scattering approximation model with importance sampling. Importance sampling is a variance reduction technique. I will focus on a couple of parameters when finding an importance sampling function. These parameters are the eccentricity and the number of hair strands. Other parameters are assumed to be constant, such as the index of refraction of 1.55, which is a completely logical value for human hair strands. This means that the importance sampling function might be less efficient for hair strands with a different index of refraction.

To find a sampling strategy, plots will be generated to show the response of the dual scattering approximation for different eccentricity values and number of occluded strands. These occluded strands are the number of strands between a point to render and the light source. More occluded strands mean that less light will reach the point in question. The response graphs are to be matched with a mathematical formula that can be inverted to a cumulative distribution form (CDF). This is necessary for efficient importance sampling. Speed gains or variance decrease tests are performed afterwards to show the performance of the importance sampling function.

The rest of this paper is divided into a background section, where the basics are explained regarding radiometry and hair rendering. Related work explains the different methods that exist to render hair. Here the Marschner model and the Dual Scattering approximation model are explained in depth, because these models are the basis for the work in this paper. After the related work, the approach will be explained on how to find the importance sampling function, followed by the results section showing the efficiency and the analysis of the multiple importance sampling function versus the standard dual scattering approximation model.

Chapter 2

Background

Hair exist in different kind of styles. According to Ward et al. [8] hair can be smooth, jagged, wavy or curly depending on the ethnic group. Three different ethnic groups are distinguished: Asian, African and Caucasian hair. A hair fiber can either have a circular or elliptical cross section. Asian hair tends to be very smooth and regular with a circular cross section, whereas African hair is very irregular and has an elliptical cross section. Caucasian hair is in between and can be a mixture of both properties.

The follicle is the active part of hair under the skin and produces keratin proteins that compose the hair material [3]. The visible part of the hair is called the hair shaft. Hair has an almost uniform cross section, natural twist and natural curvatures all along [3]. It makes the hair appear curly, straight, fuzzy, smooth, etcetera. These parameters are characteristic for the ethnic group.

A hair fiber of the human scalp consist of three layers. The outside layer is the cuticle. The cuticle is a thin sheath of protective layers that surround the inner cortex. It forms the interface between the fiber and the air. The protective sheath consist of flat cells on top of each other. Because of the overlapped arrangement the surface normal is tilted slightly from the overall normal of the fiber's surface. According to Marschner et al. [6] the surface normals are tiled by approximately 3 degrees toward the root. See figure 2.1 for a view on the cuticle scales.

The center of the hair fiber consists of the medulla: a pigmented core. The pigments give hair its color. The cortex is the core of the fiber and provides the strength for the hair fiber. The cortex is filled with keratin, contributing 90% of the total weight [8]. Keratin is a stiff material that causes hair to be easily bend and twisted, but hard to shear and stretch.

Hair consists of amorphous proteins that act as a transparent medium with an index of refraction of $\eta = 1.55$ [8]. A hair model will later be introduced that models hair fibers as dielectric cylinders where the index of refraction is important in deciding the refraction angle and the amount of
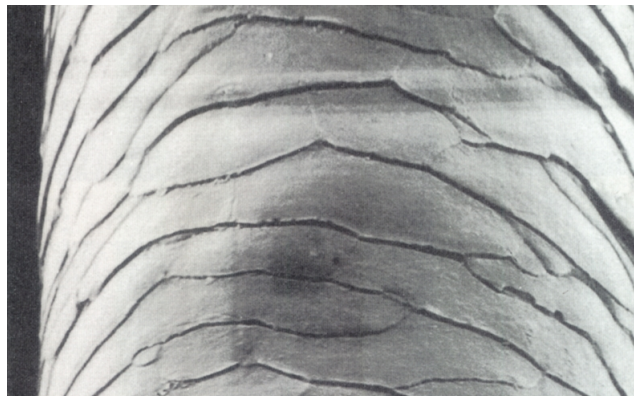
Fresnel reflection.

Figure 2.1: The tilted cuticle scales on the outside of the hair fiber.

2.1 Rendering hair

Marschner et al. [6] explain that hair rendering is a complex task, because local and global properties of hair must be taken into account. Local properties describe how light interacts with hair fibers and global properties describe the propagation of light through a volume of hair. In general, hair can be modelled explicitly or implicitly.

2.1.1 Explicit Representation

Hair research began by analyzing hair models using an explicit representation. This means that a hair model is represented as individual strands, or one-dimensional curves in three-dimensional space. Building on these foundations, researchers tried to find an efficient model to render a full head of human hair. Though several paths have been followed, modelling a full head of hair remains a challenge due to the geometric complexity and the thin nature of an individual strand coupled with the complex scattering effects and shadows that occur among the hairs [8].

2.1.2 Implicit Representation

Implicit hair representations stay away from the complexities of individual strands. With implicit representations, hair is rendered by approximating the appearance of the several strands using simpler and more efficient rendering strategies. Voxel grids, multi-layer textures or polygonal boundary representations are some of the possibilities to efficiently render a full hair model.

Implicit hair is usually modelled as a volume or polygonal boundary representation. Implicit representations work great when looking at hair from a distance, because at a distance the detail is hardly visible. Moreover, it is much faster in rendering and still giving good-looking results.

The downside of implicit representations is that it is not physically based and it is not flexible. Local scattering behaviour such as reflection and refraction, based on viewing direction and orientation of the hair strand are simplified. For physically based rendering, the explicit representation is the only way to go.

2.1.3 Geometric complexity

A human scalp may consist of over 200.000 hair strands. Some animals, such as bears might realistically be rendered with millions of hair strands. It is clear that the amount of hair fibers lead to a geometric complex challenge.

A hair fiber is naturally represented with a curved cylinder. A single hair fiber can be represented in different ways. Connected triangle strips facing the camera may be used. Triangles are easy to intersect and a strip that always faces the camera will always be intersectable.

Another strategy is to extend camera facing triangle strips, making three ribbons and attach the ends together to form a trigonal prism.

Another strategy is to make use of a cylindrical primitive. This is the most realistic solution, since hair fibers are it comes closest to how a hair fiber is physically represented. Normals are also straightforwardly find when ray-tracing a cylinder.

In this project a single hair fiber is represented as a one-dimensional curve in three-dimensional space. When rendering these curves are used to make a camera facing triangle strip to be able to ray-trace the curve.

2.1.4 Aliasing problem

A hair fiber is extremely thin. It is usually much smaller than the size of a pixel. Tracing a ray through a pixel will most likely miss the hair fiber. To be able to render a hair strand is challenging and introduces aliasing.

According to Hadap et al. [3] There are in general two strategies to perform anti-aliasing:

- Oversampling: With oversampling you cast a lot of rays through a single pixel so that enough rays hit the fiber to smooth out the aliasing effect. This is a very expensive solution, because it increases rendering time considerably For example, tracing 128 samples through a pixel could lead to a 128 times higher rendering time.

- Pixel Blending: blend the contribution of each hair fiber per pixel. This comes close to rasterization. Assuming that a curve is represented as a

one-dimensional curve in three-dimensional space, then a fiber consists of a sequence of curve points. Drawing a spline based on these curve points, one can compute the contribution at each fragment of the curve, then backprojecting on the camera plane to find out which pixel is affected and add the contribution to the pixel. Blending needs to be performed to incorporate fibers that are positioned behind each other.

Physically based rendering is based on ray-tracing, so in this project the aliasing problem is overcome by oversampling and by giving each hair fiber a certain width when rendering. Increasing the width of a hair fiber makes it easier to ray-trace, thereby reducing the need for many samples. The Renderman Shading Language (RSL) has built in functionality to render curves.

2.1.5 Mathematical Notation

The notation that is used in this thesis is the same as the one used by Marschner et al. [6] and is common in the field of hair rendering. A hair strand is represented as a one-dimensional curve in three-dimensional space. A *uvw* coordinate axis is attached to any point along the curve.

The u-axis is tangent to the hair fiber and pointing in the direction from the root toward the tip. v and w complete a right-handed orthonormal basis and are situated in the normal plane of the hair fiber. If the cross section is elliptical, then v represents the major axis and w the minor axis. The direction where the illumination is coming from is denoted by ω_i and the direction in which light is scattered is ω_r. These directions are expressed in spherical angles (θ_i, ϕ_i) and (θ_r, ϕ_r) respectively.

The longitudinal inclinations with respect to the normal plane are denoted θ_i and θ_r and are measured so that 0° is perpendicular to the hair and 90° is u and $-90°$ is $-u$. The azimuths around the hair are denoted ϕ_i and ϕ_r, measured so that v is 0° and w is $+90°$.

Derived angles are used, such as the difference angle $\theta_d = (theta_r - \theta_i)/2$. The relative azimuth $\phi = \phi_r - \phi_i$. The half-angles are $\theta_h = (\theta_i + \theta_r)/2$ and $\phi_h = (\phi_i + \phi_r)/2$. Figure 2.2 shows an overview of the axes and spherical angles.

2.2 Radiometry

It is important to understand the terminology in radiometry to get a good understanding of the theory that is explained in this report. If you are already familiar to this theory, you can skip this section. This theory is primarily meant for ones that are new to the field of rendering.
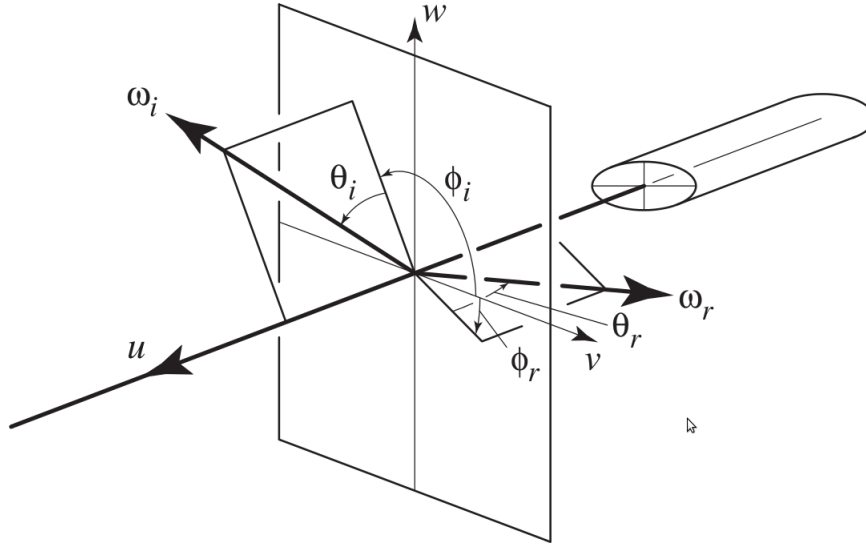
Figure 2.2: An overview of the coordinate axes and the spherical angles with respect to a hair fiber. This is the convention used in this thesis and is used by Marschner et al. and most other hair rendering algorithms. Picture taken from Marschner et al. [6].

2.2.1 Power and radiant flux

Power is the rate at which energy is transferred and is expressed in watts (W). A single watt describes the transfer of a single Joule (J) of energy per unit time (s).

A lot of electronic machines consume power, and each one does it in it's own particular way. You can think of light, heat, force, pressure, etcetera. Consider a light source that emits light particles through the scene at a certain rate. Some lights are stronger than others, meaning that the stronger light has more power and sends out the energy at a faster rate into the scene. These elementary light particles are called photons. Photons exhibit a wave-particle duality. On one side they can be treated as minuscule particles and on the other side they can be treated as waves, or more specifically: electromagnetic waves.

The rate at which a light source sends out electromagnetic waves is called radiant flux. Radiant flux Φ is the power of electromagnetic waves and describes the transfer of radiant energy (J) per unit time (s). Radiant flux is therefore also expressed in watts (W).

2.2.2 Solid Angle and Radiant Intensity

A two-dimensional angle can be thought of as drawing two lines from the center of a circle outward. Angles are represented as degrees or radians,

but radians are more convenient for mathematical purposes. A solid angle Ω is the two-dimensional angle in three dimensional space that an object subtends at a point. Consider projecting a three-dimensional object onto a unit sphere. An object that is closer to the sphere may have the same solid angle as an object that is farther away. In this case, the object that is farther is bigger than the object closer to the unit sphere, but both have the same solid angle. A solid angle is a dimensionless unit of measurement called a steradian (sr). Steradian coming from squared radian.

The radiant intensity I is a measure of the intensity of electromagnetic radiation. It can be seen as the energy flow divided by the solid angle in which it is transmitted. Radiant intensity is defined as radiant power per unit solid angle ($W \cdot sr^{-1}$).

2.2.3   Radiance versus Irradiance

Formally, irradiance E is defined as the amount of power of electromagnetic radiation per unit area incident on a surface. The unit for irradiance is watts per square meter ($W \cdot m^{-2}$).

Radiance L measures the light intensity per unit area on a surface. It measures the quantity of radiation that passes through or is emitted from a surface and falls within a given solid angle in a specified direction. Radiance is used to characterize diffuse emission. The unit of radiance is watts per steradian per square meter ($W \cdot sr^{-1} \cdot m^{-2}$).

$$L = \frac{d^2\Phi}{dA \, d\Omega \cos\theta} \approx \frac{\Phi}{\Omega A \cos\theta} \tag{2.1}$$

Figure 2.3 shows a simplified scenario of the sun shining on a surface. Irradiance is the amount of flux that is received per unit area, or in other words, the amount of sunshine impinging on the surface divided by the surface area. If we consider a rectangular bundle of light that hits the surface from a perpendicular direction ω_i, then it is obvious to see that all the light falls into an equally sized rectangle on the surface. The irradiance would be equal to the power (or wattage) of this bundle of light, divided by the surface area, assuming this is the only light that shines on the surface.

As the sun moves along the sky, the direction from which it hits the surface changes. At some point, the sunlight is coming from a more glancing direction ω_i'. If we consider the same rectangular bundle of light with size w, we notice that this bundle of light now spreads its power over a larger area. A larger area means that the irradiance becomes smaller. The same rectangular surface area does not receive the full potential power of the bundle of light anymore.

As the sun goes down, a point will eventually be reached that the direction of the sun rays will be parallel to the surface (or perpendicular to the

surface normal $\vec{n}$). In this case none of the sunlight is able to reach the surface anymore.

In reality, the irradiance is computed for an infinitisemal small area dA. If the area becomes infinitisemal small, the irradiance from direction ω_i becomes a infinitisemal small bundles as well. Therefore in a bidirectional reflection distribution function (BRDF) the irradiance is sampled for a single direction.
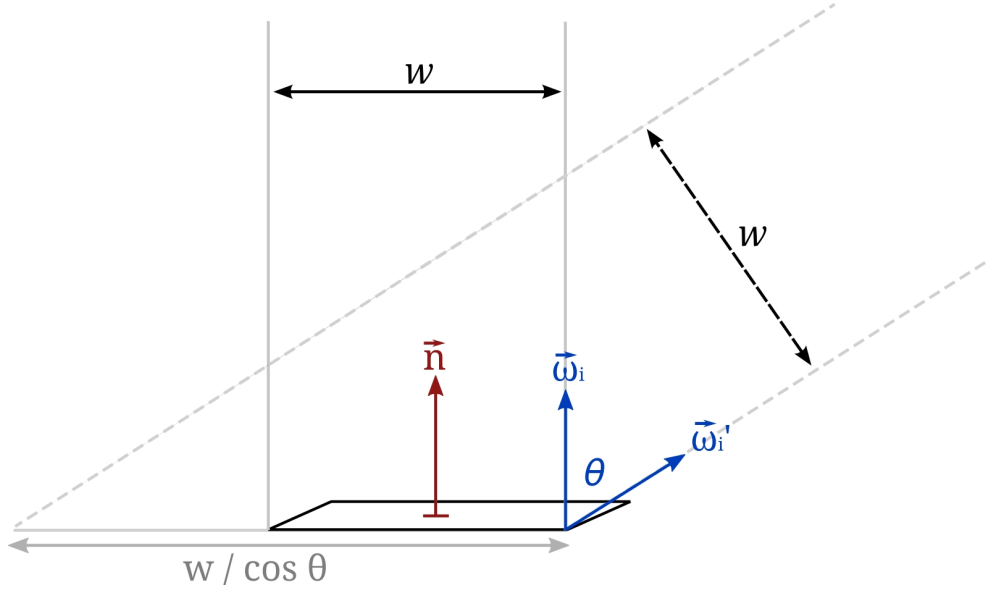

Figure 2.3: As the incoming light hits the surface at a larger angle, the irradiance decreases because the same amount of light will be spread over a greater surface area.

2.2.4 Bidirectional Reflection Distribution Function (BRDF)

When a surface is lit by a light source, part of it will scatter back into the environment. The distribution at which light is scattered back can be described by a bidirectional scattering distribution function (BSDF). If the surface is opaque and we are only taking into accounts reflection inside the hemisphere, then the reflection behaviour can be described by a bidirectional reflectance distribution function (BRDF). At some point p on the surface, the BRDF function f_r describes the relation between the amount of incoming radiance from direction w_i, $L_i(\omega_i)$, and the amount of reflected outgoing radiance in direction w_o, $L_o(\omega_o)$.

Physically based BRDFs have two important characteristics [?]:

- Reciprocity: the incoming and outgoing directions can be swapped and

11

still have the same reflection behaviour: $f_r(p, \omega_i, \omega_o) = f_r(p, \omega_o, \omega_i)$.

- Energy conservation: the total amount of energy that is reflected will always be less or equal than the amount of energy that is incident on the surface.

Physically, a BRDF describes the relation between the amount of differentiated irradiance $dE(p, \omega_i)$ and the differentiated outgoing radiance $dL_o(p, \omega_o)$.

$$f_r(p, \omega_o, \omega_i) = \frac{dL_o(p, \omega_o)}{dE(p, \omega_i)} = \frac{dL_o(p, \omega_o)}{L_i(p, \omega_i)\cos\theta_i d\omega_i} \qquad (2.2)$$

2.2.5 Bidirectional Curve Scattering Distribution Function (BCDSF)

Fibers are usually treated as one-dimensional curves. Therefore, scattering from fibers need to be described a little differently from the more familiar surface reflection [8]. As discussed in the previous section, a BRDF describes the ratio between surface radiance exiting the surface in direction ω_r, to surface irradiance falling on the surface from a differential solid angle ω_i [8].

For fibers we are not talking about surfaces, but about lengths on a curve. This means that scattering from a fiber is described with a bidirectional curve scattering distribution function (BCSDF). A BCSDF describes the ratio between curve radiance exiting the curve in direction ω_r to curve irradiance falling on the surface from a differential solid angle ω_i. It shares the same physical units, but the concept is a little different.

$$S(\omega_i, \omega_r) = \frac{dL_r(\omega_r)}{dE_i(\omega_i)} \qquad (2.3)$$

L_r is the curve radiance scattered from an infinitesimal length of fiber and E_i is curve irradiance on that portion of the fiber [6]. Curve irradiance is proportional to incoming curve radiance:

$$dE_i(\omega_i) = D L_i(\omega_i)\cos\theta_i d\omega_i \qquad (2.4)$$

Here D denotes the diameter of the fiber. So, curve irradiance is the amount of light falling on an infinitesimal small length of curve dl, times the diameter of the fiber: Ddl. Using the former equation, the scattering integral can be written as:

$$L_r(\omega_r) = D \int S(\omega_i, \omega_r) L_i(\omega_i)\cos\theta_i d\omega_i \qquad (2.5)$$

2.2.6 Rendering Equation

The rendering equation is an integral and formally describes the amount radiance leaving from a position p in direction ω_o. The radiance consists of the emitted light L_e plus the integral around the sphere to integrate all incoming light L_i from incident direction ω_i, reflecting in direction ω_o, where the BSDF is denoted by $f(p, \omega_o, \omega_i)$ indicating the contribution of incident light reflected in the outgoing direction at position p. The cosine factor is to take into account the angle with the surface (see section 2.2.3).

$$L_o(p, \omega_o) = L_e(p, \omega_o) + \int_\Omega f(p, \omega_o, \omega_i)\, L_i(p, \omega_i)\, \cos\theta_i\, d\omega_i \qquad (2.6)$$

Solving this equation is the key task for a computer graphics program. Hair fibers do not emit radiance and therefore the emitted radiance can be ignored in the rendering equation, obtaining the following equation that will be used in this thesis.

$$L_o(p, \omega_o) = L_e(p, \omega_o) + \int_\Omega f(p, \omega_o, \omega_i)\, L_i(p, \omega_i)\, \cos\theta_i\, d\omega_i \qquad (2.7)$$

2.3 Importance Sampling

Importance sampling is a variance reduction technique. The idea is to prefer samples that have more impact on the end result (i.e. the rendering) than samples that hardly have an influence. In other words, samples with a higher impact are more important to sample from, than samples that hardly have impact. By prefering samples of important directions we are converging faster to the correct end result, thereby decreasing rendering times significantly.

2.3.1 Monte-Carlo integration

Given a function $f(x)$ that we want to integrate over the range $[a, b]$. Determining the integral can be done in numerous ways. If it is possible to find the integral equation for $\int f(x)dx = F(x)$, then we could solve the integral analytically and there would be no need for Monte-Carlo integration.

In the context of physically based rendering, the integral is often too complicated to solve analytically. The Monte-Carlo integration is a relatively simple way to be able to find the expected value of an integral. Monte-Carlo integration is doing that by taking N random samples and averaging the result, thereby coming closer to the correct result. The larger the number of samples, the more accurate the result will be, eventually converging to the correct result for the integral. The following equation describes the computation of the integral F_N with the Monte-Carlo estimator **??**.

$$F_N = \frac{1}{N} \sum_{i=1}^{N} \frac{f(X_i)}{p(X_i)} \tag{2.8}$$

N represents the number of samples taken, X_i represents the i-th random sample and $p(X_i)$ is the probability density for sample X_i. If the probability density function $p(x)$ is constant, the equation becomes finding the average value and then multiplying by the size of the domain.

2.3.2 Importance sampling

It becomes interesting when the probability density function $p(x)$ is not constant for all samples. By giving certain samples a higher probability and other (less important) samples a lower probability, we can converge faster to the correct result by using less samples.

The idea behind importance sampling is to draw samples from the probability distribution function (PDF). There are different techniques to draw samples from a PDF as explained in the book by Pharr et al. **??**. Possible techniques are inversion sampling, in which the normalized cumulative distribution function (CDF) is computed, then inverted and used with a uniform random variable $\Xi \in (0, 1]$ to obtain a sample X. Other techniques are rejection sampling.

It is easy to see that the better the fit of the PDF with the function $f(x)$, the better the drawn samples and the faster we converge to the correct result. If $f(x) = p(x)$ we are talking about perfect importance sampling, the most ideal case. However, it is not always possible to invert $f(x)$. If we can find a PDF that is still a close fit to $f(x)$ but is possible to invert, then we still have a better sampling technique compared to uniform sampling.

Other techniques are possible as well, such as rejection sampling, which is described indetail in Pharr et al. **??**.

2.3.3 Multiple importance sampling

Sometimes we end up with a function that can be written as the product of multiple functions $f(x)g(x)$, each of which has an easy to sample from PDF $p_f(x)$, belonging to $f(x)$ and $p_g(x)$ for $g(x)$.

If two sampling distributions $p_f(x)$ and $p_g(x)$ are used to estimate the value of $\int f(x)g(x)dx$, you cannot just average the results by taking N samples from $p_f(x)$ and M samples from $p_g(x)$ and average the result, because variance is additive. The way how to do it is by using the new Monte-Carlo estimator for multiple importance sampling (MIS) stated in **??**:

$$\frac{1}{n_f} \sum_{i=1}^{n_f} \frac{f(X_i)g(X_i)w_f(X_i)}{p_f(X_i)} + \frac{1}{n_g} \sum_{j=1}^{n_g} \frac{f(Y_j)g(Y_j)w_g(Y_j)}{p_g(Y_j)} \tag{2.9}$$

where w_f and w_g are weighting functions.

$$w_s(x) = \frac{n_s p_s(x)}{\sum_i n_i p_i(x)} \qquad (2.10)$$

Chapter 3

Related Work

3.1 Hair Rendering Overview

The explicit representation of hair provides the most physically accurate results, because simulating the scattering events fiber by fiber is also what happens in nature. Considering a single hair fiber, models have been proposed to render such a fiber. To increase the realistic appearance of hair fibers, more fibers should be taken into account. This leads to the concept of multiple fiber scattering. Multiple fiber scattering is analogous to subsurface scattering in solid materials and therefore necessary to increase the level of realism. Ward et al. [8] provides a good overview on the different models in hair rendering in general.

In this section, related work regarding the development of hair models is explained, followed by an in-depth treatment of the most relevant work related to the research in this paper.

3.1.1 Single fiber scattering

Kajiya and Kay [5] provided one of the first widely used hair scattering model that was designed to render fur. Fur usually refers to a dense coat of fine and soft hair. Their idea was that fine hair geometry should not be represented with complex geometry which leads to aliasing effects, but with texels. A texel is a three-dimensional texture map intended to represent a highly complex collection of surfaces contained within a defined volume [5].

The rendering of the hair model was based on a diffuse and specular component. The diffuse component is obtained by simply integrating a Lambert surface along one half of the cylinder facing the light source. The specular component is based on the Phong model in which light is reflected at a mirror angle along the tangent. Since the normals on the cylinder point in directions perpendicular to the tangent, the reflected light forms a cone whose angle at the apex is equal to the angle of incidence [5]. The Kajiya and Kay model is clearly an ad-hoc model where hair fibers are treated as

opaque cylinders, limiting the realism of the model.

The Kajiya and Kay model lacks directionality, meaning that hairs are fully lit independent on the light direction or eye position. Goldman [1] was interested in reflection and transmission and increased directionality by introducing two new attenuation factors. These attenuation factors can be used to tune the relative transmissivity and reflectivity of a hair. It does this by computing a value f_{DIR} that is multiplied with the contribution of the Kajiya and Kay model.

Marschner et al. [6] improved the Kajiya and Kay model substantially by proposing the most physically based hair scattering model at that time. Their model makes two improvements to Kajiya and Kay's model: it predicts the azimuthal variation in scattered light based on the ray optics of a cylinder, and it accounts for the longitudinal separation of the highlight into surface-reflection, transmission, and internal-reflection components that emerge at different angles [3]. The Marschner model is described in detail in section 3.2.

3.1.2 Multiple fiber scattering

For fully realistic results, light that reflects from hair to hair, or multiple scattering, must be accounted for [8].

Multiple fiber scattering extends single fiber scattering to include the scattering effects between seperate hair strands. A single fiber scattering model can be used as the basis for multiple fiber scattering. For example, if the Marschner model is used for single fiber scattering in combination with path tracing along all the hairs in hair model, we obtain the result for multiple fiber scattering. Path tracing is realistic, but given the geometric complexity of a hair model, a very time consuming process. More efficient multiple fiber scattering models should be devised.

Photon mapping methods can reduce per-frame rendering times from days, required for path tracing methods, to hours [8]. Photon mapping is a practical approach for computing global illumination in complex environments. Photon mapping is introduced by Henrik Wann Jensen [4] and it is, in general, a two-step approach. The first pass in the method is constructing the photon map by emitting photons from the light sources in the model and storing these in the photon map as they hit surfaces [4]. The collection of photons distributed in the photon map, can be seen as a rough representation for the amount of light in the scene. The second step is that this information from the photon map is used to render the scene.

For multiple scattering in hair models, Moon and Marschner [7] developed a model using a photon mapping approach. In the first pass, particles are

17

traced from light sources into the hair volume and followed through multiple scattering events, and their positions and directions are stored into a 5D hierarchical data structure to record the flow of particles through space [7]. In the second pass a density estimate is performed simultaneously in position and direction to estimate the radiance arriving at a hair from a particular direction. This photon mapping approach leads to similar results compared to path tracing, but the biggest drawback is that it requires high resolution photon maps (memory usage) and the method is not interactive.

The Dual Scattering approximation is a direct extension on top of Marschner and doesn´t have the drawbacks of photon mapping approaches. The dual scattering approximation splits up the compensation in a global and a local scattering component. The global scattering component computes the amount of irradiance reaching a certain position in the hair model. The local scattering component uses the computed irradiance to compute the scattering effects in the direct neighbourhood of the position to be rendered. More in-depth theory is provided in section **??**.

3.2 Marschner model

The biggest drawback of Kajiya and Kay [5] is that their scattering model is not based on physical measurements. Instead, it uses a simple ad-hoc term with a constant linear highlight. Marschner et al. [6] proposed a physically based scattering model for single fiber scattering. The single fiber scattering model, or Marschner model, forms the basis for the dual scattering approximation and will be discussed in detail.

3.2.1 Observations

In order to come up with a physically based scattering model for single hair fibers, Marschner et al. devised a setup to capture the response of light scattered against a hair fiber.

They illuminated individual hairs with a narrow beam and measured the scattered light in various directions, using a setup based on a four-axis goniometer that positioned a light source and a CCD camera at arbitrary directions from the sample [6]. Their measurements show a couple of distinct characteristics for human hair.

Longitudinal variation

Stamm et al. and Bustard and Smith measured the scattering behaviour in the incidence plane. This is the 2D slice for which the hair fiber is coplanar with the source and detector. Marschner et al. did the same measurements and placed a light source under a direction of positive and negative 45 degrees with the hair fiber ($\theta_i = +/-45°$). See figure 3.1 for the measured responses.

Observations show that synthetic hair has a highlight that appears exactly at the specular direction ($\theta_r = -\theta_i$), but for real hair fibers the specular highlight is shifted toward the root of the hair fiber. This is due to the tilted cuticle scales that have a surface orientation that is shifted by approximately 6 to 8 degrees from the ideal cylinder surface normal. This highlight is the result of scattering against the surface of the hair fiber. It is called the primary specular highlight and appears as having the color of the light source.
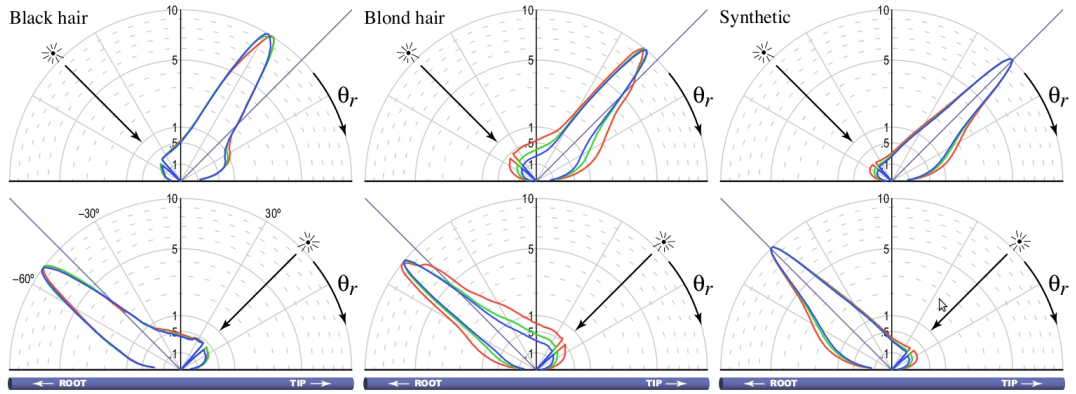

Figure 3.1: The scattering behaviour in the incidence plane (longitudinal scattering). For human hair the specular reflection is shifted towards the root by a few degrees. For synthetic hair no shifted highlight is visible, because synthetic hair doesn't consist of tilted cuticle scales.

Another observation is that blond hair has a coloured secondary peak. This can be seen by the red response that is slightly higher compared to the blue and red response. The secondary peak can be explained by internal scattering. Consider the hair fiber as a cylinder; when light enters the cylinder, the light will first refract, then propagates through the core of the fiber and bounces back against the other end of the fiber. When leaving the fiber, the light refracts again. This reflection and refraction behaviour causes the deviation from the primary specular highlight. During its travel, light propagated through the center of the hair fiber, where the pigments are. These pigments absorb part of the energy in different wavelengths. This is how the secondary peak gets its colour.

Furthermore, Marschner et al. [6] noted that as the scattering angle increases, the secondary highlight fades out, while the primary highlight maintains more constant amplitude. Both peaks maintain approximately constant width and at high angles the primary highlight becomes a sharp peak that is prominent very close to the specular direction.
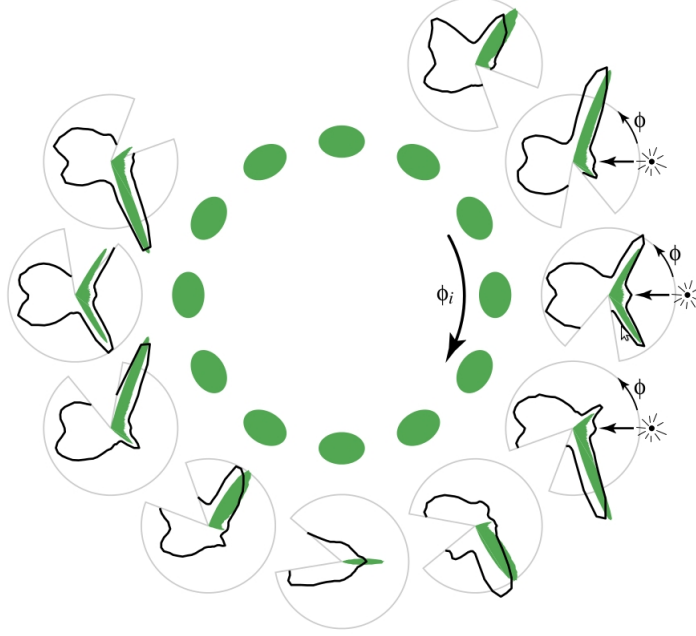
19

Azimuthal variation

Figure 3.2: Measurements of azimuthal scattering (scattering in the normal plane). The light source is shining from the right, while the hair fiber is rotated. The green ellipse is the cross section of the fiber for different measurements with increasing rotations of the fiber. Figure taken from Marschner et al. [6].

Azimuthal variation is measured by placing the light and detector in the plane that is perpendicular to the hair fiber: the normal plane. In figure 3.2 plots are displayed that show the azimuthal scattering response with varying ϕ_i and ϕ_r. The setup is that the light source is fixed (targeted from right to left) and the hair fiber is rotated.

In this normal plane setup, it is clearly visible that there are two bright out-of-plane peaks. Out of plane, because the response is captured at $\theta_r = 10$ degrees, due to the tilted cuticle scales discussed before. These peaks are called glints.

The glints change considerably in brightness and position as a function of θ_i, meaning that the hair is not rotationally symmetric [6]. This is because the hair is eccentric and has an elliptical cross section. More generally, the evolution of the peaks as the fiber rotates appears similar to the internal reflection from a transparent elliptical cylinder [6].

Figure 3.2 also shows a strong transmission component. This is light

that passes through the hair fiber and leaving on the other side of the fiber as seen from the light source. This means that the Marschner hair model takes three scattering modes into account. R stands for reflection and T for transmission:

- R: Specular reflection that is deviated slightly from the perfect specular direction, due to the cuticle scales.

- TT: Transmission component that enters the fiber, propagates through it and leaves the fiber at the other end.

- TRT: Internal reflection, that enters the fiber, scatters back and leaves again at the same side as where it entered.

More scattering modes are possible as well, such as TRRT or TRRRT. These events are ignored, because their contributions become negligible small due to loss of energy after that many reflection events. Instead, Marschner et al. [6] suggests to add a little diffuse color for better looking results. In figure 3.3 an image is shown with the three scattering components clearly visible.

3.2.2 Model

There are properties that have been used in previous work on scattering from fibers ([Marcuse 1974; Adler et al. 1998; Mount et al. 1998]):

- A ray that enters a dielectric cylinder at a particular angle to the axis will always exit at the same angle, regardless of the sequence of reflections and refractions it undergoes.

- The dependence of the scattered distribution can be analysed by examining only the projection into a plane perpendicular to the hair.

Based on the observations described in the previous subsection and the theory here, Marschner et al. came up with a model that is divided into a longitudinal scattering component M and an azimuthal scattering component N. Each scattering mode (R, TT and TRT) has it's own component, resulting in the following scattering model:

$$S(\omega_i, \omega_r) = M_r \tag{3.1}$$

S depends on incoming and outgoing angles ω_i and ω_r, but can be reduced to a 2D scattering function, since the scattering model makes use of the difference angles θ_h and ϕ.

Figure 3.3: An image from Gray [2] showing a female with brown hair. The three scattering modes: R, TT and TRT contributions are visible in the hair. Glints give hair it's characteristic texture.

Longitudinal Scattering Function

Using the first property of scattering from fibers, it can be derived that the angle of incidence will be the same as the angle of reflection ($\theta_i = -\theta_r$). There are two deviations that cause the reflection to not be exactly in the specular direction (see section 3.2.1). First, the surface of hair fibers are rough, causing a spread of reflected light instead of a mirror reflection. Secondly, the cuticle scales of the hair fiber cause a 6 to 8 degrees deviation from the perfect specular direction.

Marschner et al. approximated the longitudinal scattering function M by a unit-integral zero-mean Gaussian function $g(\beta, x)$, where β equals the standard deviation.

The resulting longitudinal scattering functions are displayed in figure 3.4.

By varying the standard deviation β, the spread of the longitudinal scattering component can be adjusted to simulate the rough surface of hair fibers. α deviates the peak from the specular direction by shifting the gaussian dis-

$$M_R(\theta_h) = g(\beta_R, \theta_h - \alpha_R)$$
$$M_{TT}(\theta_h) = g(\beta_{TT}, \theta_h - \alpha_{TT})$$
$$M_{TRT}(\theta_h) = g(\beta_{TRT}, \theta_h - \alpha_{TRT})$$

Figure 3.4: Longitudinal scattering functions for the Marschner model.

tribution. Marschner et al [6] provided some typical values for α and β (see table 3.1).

Parameter	Description	Typical value
α_R	Longitudinal shift for R lobe	-10° to -5°
α_{TT}	Longitudinal shift for TT lobe	$-\alpha_R/2$
α_{TRT}	Longitudinal shift for TRTlobe	$-3\alpha_R/2$
β_R	Longitudinal spread for R lobe	5° to 10°
β_{TT}	Longitudinal spread for TT lobe	$\beta_R/2$
β_{TRT}	Longitudinal spread for TRT lobe	$2\beta_R$

Table 3.1: Typical values for parameters for the longitudinal scattering function. Taken from Marschner et al. [6]

Azimuthal scattering Function

The azimuthal scattering component requires more thought, since different scattering paths inside the circular cross section need to be considered.

Scattering from a dielectric circle is well studied. Consider a parallel beam incident on a circular cross section at an offset h from the center. A parallel beam incident on the center of a circle means that $h = 0$. A value of $h = +/-1$ indicates that the parallel beam is glancing the edges of the circle. Using the offset h, the angle of incidence γ_i can be computed using the following equation:

$$\sin\gamma_i = h \quad \Leftrightarrow \quad \gamma_i = \arcsin h$$
$$\eta \sin\gamma_t = h \quad \Leftrightarrow \quad \gamma_t = (\arcsin h)/\eta$$

A ray that is incident on the unit circle can be traced as it refracts and reflects through the circle. The exit angle is not only dependent on the incidence angle (or offset from the center), but also on the number of scattering events. The number of scattering events p equals 1 for the reflection case, 2 for transmission (TT) and 3 for internal reflection (TRT). The exit angle can then be calculated as follows:

$$\phi(p, h) = 2p\gamma_t - 2\gamma_i + p\pi \tag{3.2}$$

The figure from Marschner et al. provides a good overview on the possible scattering events and the relation between the scattering angles.

Consider rendering a scene using ray tracing and that a particular camera ray is incident on a hair fiber. To find the contribution for the rendered image, we need to find all the paths that contribute to scattering in the direction of the camera ray. These paths are found by solving for roots. The R and TT cases have exactly one root and TRT has either one or three roots. The h values for these paths are found by solving for the roots of the function $\phi(p, h) - \phi = 0$. Finding the roots requires solving a cubic equation, which is explained deeper in Marschner et al. [6]. The roots are denoted by $h(p, r, \phi)$ where different values of r denote different roots.

Attenuation has to be taken into account as well. Attenuation occurs because of reflections, refractions and absorption. The attenuation for reflections and refractions are computed using the Fresnel equation. The Fresnel equation takes a parallel and perpendicular index of refraction (η' and η'' respectively). Absorption takes place when a ray propagates through the hair fiber. The length of each internal path segment is computed by applying the law of cosines. According to [], the formula given in Marschner et al. is wrong. This equation should be as followed:

$$l = \frac{2r\cos\gamma_t}{\cos\theta_t} \text{ with } \theta_t = -sgn(\theta_i)\arccos((\eta''/\eta')\cos\theta_i) \tag{3.3}$$

Here l denotes the length of a single internal path segment for the TT case. For TRT, the length doubles. r is the radius of the hair fiber and is a setting provided by the user. Absorption is denoted by $T(\sigma_a, h)$ where σ_a is the absorption coefficient. It describes the amount of absorption per unit length through the hair fiber. It follows straightforwardly that the absorption is computed as $T(\sigma_a, h) = \exp(\sigma_a l)$. The normal plane scattering function N_p can now be described and is shown in equation 3.4 be described.

$$A(0, h) = \text{Fresnel}(\eta', \eta'', \gamma_i)$$
$$A(p, h) = (1 - \text{Fresnel}(\eta', \eta'', \gamma_i))^2 \cdot \text{Fresnel}(\frac{1}{\eta'}, \frac{1}{\eta''}, \gamma_t)^{p-1} \cdot T(\sigma_a, h)$$

The normal plane scattering function for a given number of path segments p (1, 2 or 3) is given in equation 3.4.

$$N_p(p, \phi) = \sum_r A(p, h(p, r, \phi)) \cdot \left| 2\frac{d\phi}{dh}(p, h(p, r, \phi)) \right|^{-1} \tag{3.4}$$

Glints

Because the theory is based on smooth surfaces, the normal plane scattering function N_p for the TRT scenario produces singularities with infinite intensity [6]. These singularities are called caustics and is light that bundles together after a sequence of reflections and refractions. In reality, these caustics are bright spots of light that originate after a sequence of reflections and refractions. Think about light propagating through a wine glass for example. These infinite singularities are removed by replacing it with a smooth Gaussian lobe centered at the location of the caustic. This changes the normal plane scattering function for the TRT case. Marschner et al.[6] provides more detail into how the scattering function changes.

Taking into account eccentricity

Changing refractive index has effects that are qualitatively similar to changing eccentricity [6]. In order to simulate eccentricity, the refractive index is computed based on the value of eccentricity a. The equation can be found below. More detail is in Marschner et al's paper [6].

$$\eta_1^* = 2(\eta - 1)a^2 - \eta + 2 \tag{3.5}$$

$$\eta_2^* = 2(\eta - 1)a^{-2} - \eta + 2 \tag{3.6}$$

$$\eta^*(\phi_h) = \frac{1}{2}\left((\eta_1^* + \eta_2^*) + \cos(2\phi_h)(\eta_1^* + \eta_2^*)\right) \tag{3.7}$$

Marschner model

From the description above we can now describe the complete Marschner scattering model $S(\omega_i, \omega_r)$.

$$
\begin{aligned}
S(\phi_i, \theta_i; \phi_r, \theta_r) &= M_R(\theta_h)N_R(\phi)/\cos^2\theta_d \\
&+ M_{TT}(\theta_h)N_{TT}(\phi)/\cos^2\theta_d \\
&+ M_{TRT}(\theta_h)N_{TRT}(\phi)/\cos^2\theta_d
\end{aligned}
$$

Here the longitudinal functions N_x are placeholders for the normal plane scattering function N_p:

$$
\begin{aligned}
N_R(\phi) &= N_p(0, \phi) \\
N_{TT}(\phi) &= N_p(1, \phi) \\
N_{TRT}(\phi) &= N_p(2, \phi)
\end{aligned}
$$

3.2.3   Evaluation

The advantage of the Marschner hair model is that it is based on physical observations. Compared to previous approaches this is a huge win. Finding the roots for a given direction is slow, but can be dealt with by using precomputed tables.

The Marschner hair model focuses on single fiber scattering and to render realistic hair volumes, multiple fiber scattering needs to be taken into account. Path tracing or photon mapping are possible approaches, but take a lot of time or require an extensive amount of memory. Another drawback is that from own calculations, the Marschner model is not energy conserving. Especially for very wide angles, the reflections will be relatively high.

3.3   Dualscattering Approximation

Multiple scattering is a key factor in the realistic rendering of hair, especially for dense light colored hair volumes (such as blond hair). The relative amount of absorption by light colored hair types is fairly low, so this means that light undergoes many scattering interactions inside the hair volume before the contribution is reduced to an amount that can be neglegible. The high geometric complexity of hair models coupled with the compexity of the light interaction in hair volumes makes computing the multiple scattering effect difficult **??**. Difficult to an extent that path-tracing is not a feasible solution, because it requires too much time and too many samples to reduce the noise and come to an acceptable rendering.

The dual scattering approximation, proposed by Zinke et al. **??** splits the multiple scattering computation in two components: global multiple scattering and local multiple scattering. The global multiple scattering component aims to compute the light traveling through the hair volume and reaching the neighborhood of the point of interest, while local multiple scattering accounts for the scattering events within this neighborhood **??**.

Starting from the general rendering equation and ignoring the position component in the BSDF description as is common for material definitions, because materials usually behave the same irrespective of position, we obtain the following equation.

$$L_o(x, \omega_o) = \int_\Omega L_i(x, \omega_i) f_s(\omega_i, \omega_o) \cos \theta_i d\omega_i \qquad (3.8)$$

This can be interpreted as the radiance in outgoing direction ω_o at a position x, equals the integral around the sphere (Ω) of incident directions ω_i multiplied by the BSDF factor. It is not hard to see that the integration is a recursive process, and to find the incident radiance coming from direction ω_i, another integration is needed from another point x' in outgoing direc-

tion $\omega'_o = -\omega_i$. The dualscattering approximation simplifies this process by defining the incident radiance as

$$L_i(x, \omega_i) = \int_\Omega L_d(\omega_d)\Psi(x, \omega_d, \omega_i)d\omega_d \qquad (3.9)$$

where L_d is the incident radiance from outside the hair volume from direction ω_d (assuming distant illumination), and $\Psi(x, \omega_d, \omega_i)$ is the multiple scattering function denoting the fraction of light entering the hair volume from direction ω_d that is scattered inside the hair volume and finally arriving at point x from direction ω_i **??**.

The main concept behind the dual scattering method is to approximate the multiple scattering function as a combination of two components. The global multiple scattering function Ψ^G is used to compute the irradiance arriving at the neighborhood of point x inside the hair volume, and the local multiple scattering function Ψ^L approximates the multiple scattering of this irradiance within the local neighborhood of x **??**. This results in the following equation, central to the dual scattering approximation model.

$$\Psi(x, \omega_d, \omega_i) = \Psi^G(x, \omega_d, \omega_i)(1 + \Psi^L(x, \omega_d, \omega_i)) \qquad (3.10)$$

The global multiple scattering is thus responsible for gathering the irradiance from outside the hair volume and taking into account the scattering effects in the hair volume, to deliver an approximate amount of irradiance arriving at point x. It is important to see that the global multiple scattering removes the need to do extensive path tracing through the hair volume.

The local multiple scattering is more in line with the Marschner model. Given the irradiance at point x, calculate the scattering effect of the local neighbourhood. In extreme terms, a neighborhood consisting of a single fiber boils down to evaluation the Marschner model.

3.3.1 Global Multiple Scattering

The global multiple scattering function Ψ^G gathers the irradiance from outside the hair volume, thereby taking into account the scattering events within the hair volume. The global multiple scattering is defined as follows by Zinke et al. **??**

$$\Psi^G(x, \omega_d, \omega_i) \approx T_f(x, \omega_d)S_f(x, \omega_d, \omega_i) \qquad (3.11)$$

The global multiple scattering Ψ^G is the multiplication of forward transmittance T_f and the average forward scattering spread S_f. The transmittance accounts for the amount of hairs in between the light source and the point to be shaded. The average forward scattering spread takes into account the loss of energy due to spreading of the light after each scattering event.

Forward Scattering Transmittance

In this work the global irradiance is computed by using a combination of ray shooting together with a voxel grid. Before rendering, a voxel grid is generated based on the hair model. Each voxel cell contains the density of the hairs in question. This is computed by traversing each hair fiber and storing the distance of the hair fiber segment in the voxel cell. In this way, cells that contain a lot of hair fibers, do have a higher density value.

When finding the irradiance at a position x in direction ω_i, a ray is shot in the direction of the light source. This ray is linearly ray-marched and for each position along the ray, the density value is looked up in the voxel cell. In this way, the global density value is computed for a specific direction ω_i. The density factor can then be translated to the number of hair strands, by dividing the density by the volume of a voxel cell. In this way we gathered n, the number of hair strands in between the shading pointy x and the light in direction ω_i.

The forward scattering transmittance for the dual scattering method **??** is defined as follows

$$T_f(x, \omega_d) = d_f(x, \omega_d) \prod_{k=1}^{n} a_f(\theta_d^k) \tag{3.12}$$

where d_f is the forward scattering density factor, which is a constant between $[0, 1]$ and usually set to 0.7. This factor is a tweaking variable that can be changed dependent on the denseness of a hair volume. $a_f(\theta_d^k)$ is the average forward scattering attenuation at the k-th scattering event, which is computed in a precomputation step by integrating over all possible directions in the hemisphere and averaging the amount of forward scattered radiance. See the dual scattering method for more details **??** or the efficient implementation of the dual scattering model in RenderMan by Sadeghi and Tamstorf **??** for a more hands on approach.

In this work, a simplification is used by usng a constant orientation for all k scattering events, under the assumption that we are dealing with human hair fibers that are locally similar in orientation. This means equation 3.13 can be simplified to the following equation.

$$T_f(x, \omega_d) = d_f(x, \omega_d) a_f(\theta_d)^n \tag{3.13}$$

Forward Scattering Spread

The spread function approximates the final angular distribution of front scattering light to find the probability of radiance coming to the point x from direction ω_i **??**. Because of the wide azimuthal scattering property of hair fibers, front scattered radiance quickly becomes isotropic in the azimuthal direction after only a few scattering events. For longitudinal scattering front

scattered light is still anisotropic. The spread function is therefore split up into an isotropic azimuthal component $(1/\pi)$ and an anisotropic longitudinal component described by a gaussian function g.

$$S_f(x, \omega_d, \omega_i) = \frac{s_f(\phi_d, \phi_i)}{\cos \theta_d} g(\theta_d + \theta_i, \sigma_f^2(x, \omega_d)) \tag{3.14}$$

where s_f is $1/\pi$ for forward scattering directions and zero for backward scattering. $\sigma_f^2(x, \omega_d$ is the total variance of forward scattering in the longitudinal direction. This is defined by the Marschner model as the squared standard deviation β^2 and is dependent on the longitudinal angle. Simplifying again by taking a constant θ_d gives us a single multiplication of number of hair strands multiplied by the longitudinal variance.

$$\sigma_f^2(x, \omega_d) = \sum_{k=1}^{n} \beta_f^2(\theta_d^k) \approx n \cdot \beta_f^2(\theta_d) \tag{3.15}$$

3.3.2   Local Multiple Scattering

The local multiple scattering function Ψ^L accounts for the multiple scattering events within the neighborhood of the point x. Since light paths that go through only forward scattering are included in the global multiple scattering function, light paths of the local multiple scattering function must include at least one backward scattering.

Because of backward scattering, the local multiple scattering is mostly smooth with subtle changes over the hair volume **??**.

The dual scattering model the local multiple scattering and the BCSDF of the hair fibers, approximating the result with a density factor d_b and backscattering function.

$$\Psi(x, \omega_d, \omega_i) f_s(\omega_i, \omega_o) \approx d_b(x, \omega_d) f_{\text{back}}(\omega_i, \omega_o) \tag{3.16}$$

The density factor d_b is a constant in the range $[0, 1]$, usually set to 0.7 approximating the density of the hair volume. The denser the hair, the stronger the backscattering event contributes to the result.

The backscattering is approximated with a material function f_back

$$f_{\text{back}}(\omega_i, \omega_o) = \frac{2}{\cos \theta_d} A_b(\theta_d) S_b(\omega_i, \omega_o) \tag{3.17}$$

Average Backscattering Attenuation

The average backscattering attenuation takes into account the attenuation in the local neighborhood of a point x. Since the global multiple scattering component already takes into account the forward scattering (meaning no backscatter events), we only need to deal with at least 1 backscatter event.

Light coming from a light source, passing through the fiber at point x, needs an odd number of backscattering events for light to travel back to point x. The even number of backscattering events are ignored, since they are not directed to point x. Also, the dual scattering method ignores the contribution for more than three backscattering events, because their contribution becomes negligible low to the rendering result.

If we denote $a_b(\theta_d)$ as the average backscattering attenuation and $a_f(\theta_d)$ as the average forward scattering attenuation (described in the previous section), then the average backscattering for a single backscattering event A_1 can be computed as the attenuation of a single backscatter event, multiplied by the sum of the infinite series of forward scattering attenuations. The same holds for the average backscattering attenuation for three backscattering events A_3, but now the possible paths are not a single sum anymore, but multiple sums to obtain the permutation of possible paths, dependent on where the backscattering event occurs in the sequence of forward scattering attenuations.

$$A_1(\theta_d) = a_b \sum_{i=1}^{\infty} a_f^{2i} = \frac{a_b a_f^2}{1 - a_f^2} \tag{3.18}$$

$$A_3(\theta_d) = a_b^3 \sum_{i=1}^{\infty} \sum_{j=0}^{i-1} \sum_{k=j+1}^{\infty} a_f^{2(i-j-1+k)} = \frac{a_b^3 a_f^2}{(1 - a_f^2)^3} \tag{3.19}$$

$$A_b(\theta_d) = A_1(\theta_d) + A_3(\theta_d) \tag{3.20}$$

where A_b is the average backscattering attenuation for 1 and 3 backscattering events. Figure **??** provides a graphics representation of the backscattering events and how they are directed with respect to position x.

(picture here)

Average Backscattering Spread

The average backscattering spread takes into account the loss of intensity, due to spreading of the light after backscattering events occur. This is similar to forward scattering events. The dual scattering method **??** presents the average backscattering spread $S_b(\omega_i, \omega_o)$ as

$$S_b(\omega_i, \omega_o) = \frac{s_b(\phi_i, \phi_o)}{\cos \theta} g(\theta_o + \theta_i - \Delta_b(\theta_d), \sigma_b^2(\theta_d)) \tag{3.21}$$

where s_b equals $1/\pi$ for backward scattering directions and zero for forward scattering, $\Delta_b(\theta_d)$ is the average longitudinal shift caused by the scattering events.

The spread is modeled as a single gaussian function. It is important to notice that Δ_b represents the average mean and σ^2 represents the average

30

variance, thereby taking into account the multitude of possible forward and backward scattering events.

The average longitudinal shift Δ_b and average longitudinal standard deviation σ_b for backscattering can be precomputed by averaging over all directions. See the dual scattering method **??** for more details and **??** for a more hands on approach.

Chapter 4

Approach

Here comes the approach

Chapter 5

Results

5.1 Hair blocks with different density

As an indication to see the effects of using the voxel grid. The following images show. Renderings of cubes with different densities. The left cube is less dense than the right cube. If the cube has a higher density (e.g. more hairs), then more light is scattered around through the model, leading to a darker appearance as you view deeper in the cube.

The cubes are rendered with Pixar's Renderman. The size of cubes are 5x5x5 and are placed on the horizontal plane at Y = 0.

5.2 Cornwell Scene

The following images show the effects of the dual scattering algorithm for the well-known cornwell scene. The scene consists of 4 walls: a red wall to the left, a green wall to the right, a gray wall in front and a gray wall behind the camera. The wall behind the camera influences the scene, due to scattered light that reflects back into the visible part of the scene. The red diffuse sphere is present as a reference sphere.

5.3 Evaluation Strategy

To evaluate the multiple importance sampling strategy of the dual scattering approximation, we need to render different types of scenes to be able to see that the importance sampling strategy is more efficient that the standard dual scattering approximation. By taking a fixed number of samples for the integration, we expect that the importance sampling strategy will be equally fast in terms of computation speed compared to the non-importance sampling variant. However, the importance sampling strategy should generate an image that is less noisy than the standard dual scattering approximation algorithm using the same number of samples.
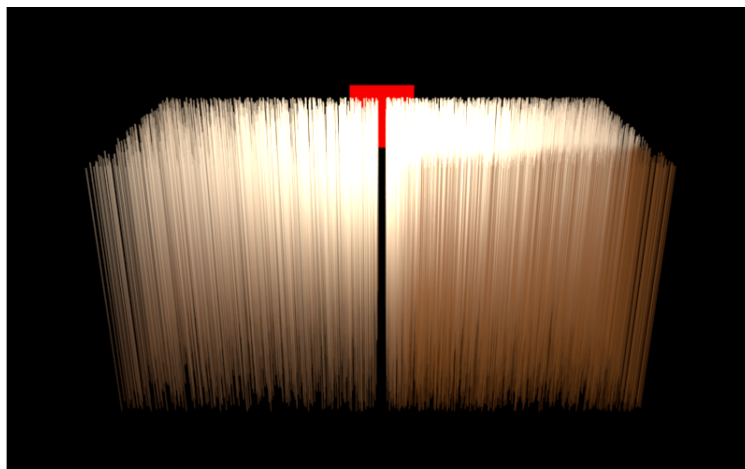
Figure 5.1: Left hair block contains 1500 hairs, versus the right hair block, that contains 3000 hairs.
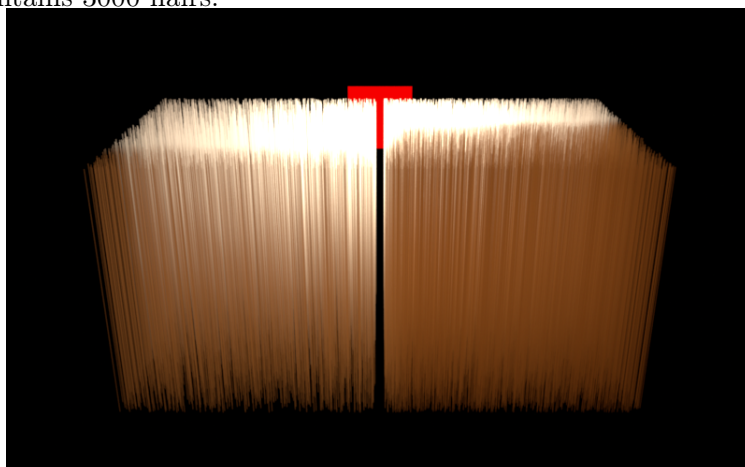

Figure 5.2: Left hair block contains 3000 hairs, versus the right hair block, that contains 6000 hairs.
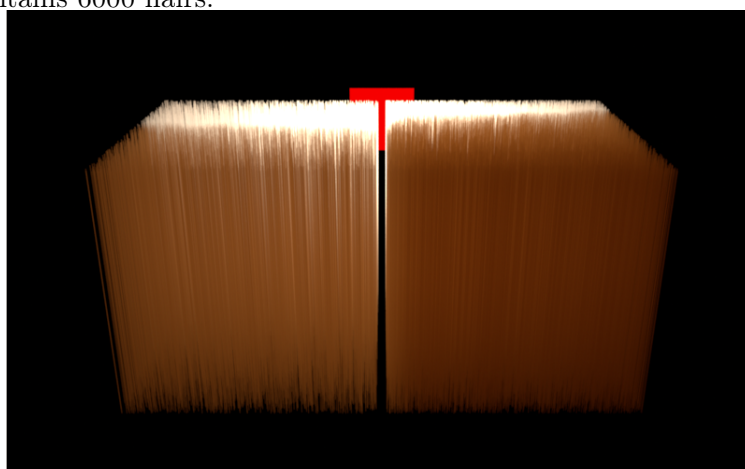

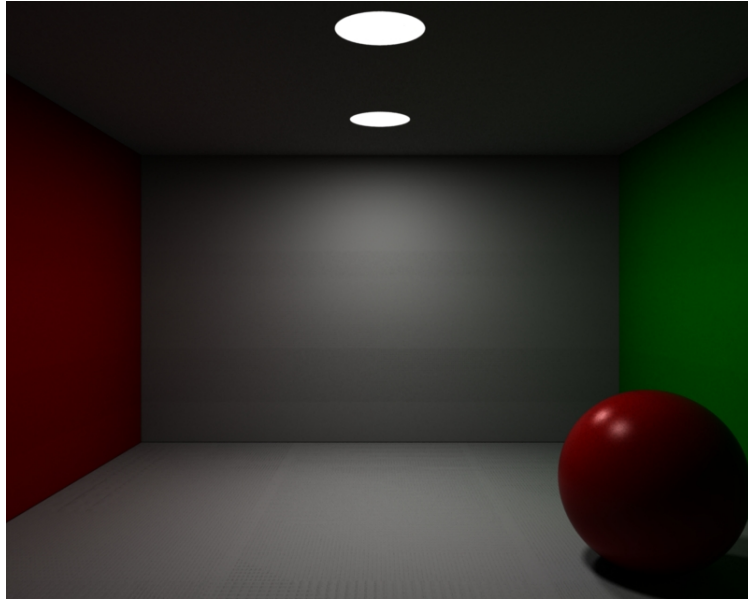Figure 5.3: Left hair block contains 6000 hairs, versus the right hair block, that contains 12000 hairs.

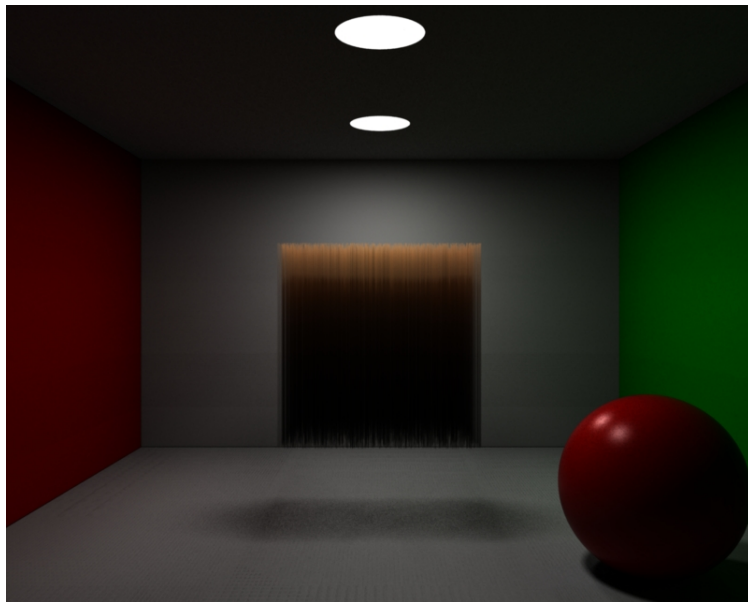Figure 5.4: Cornwell reference scene without the hair block.

Figure 5.5: Cornwell reference scene with a uniformly sampled hair block block.

Chapter 6

Conclusion

Chapter 7

Appendix

Bibliography

[1] Dan B. Goldman. Fake fur rendering. In *Proceedings of the 24th Annual Conference on Computer Graphics and Interactive Techniques*, SIGGRAPH '97, pages 127–134, New York, NY, USA, 1997. ACM Press/Addison-Wesley Publishing Co.

[2] J. Gray, R.P.R. Dawber, C. Gummer, Hairdressing Training Board, and Procter & Gamble Haircare Research Centre. *The World of Hair: A Scientific Companion*. Hairdressing Training Board. Macmillan Publishers Limited, 1997.

[3] Sunil Hadap, Marie-Paule Cani, Florence Bertails, Ming Lin, Kelly Ward, Stephen R. Marschner, Tae-Yong Kim, and Zoran Kacic-Alesic. *Strands and Hair: Modeling, Animation, and Rendering*, volume 33. ACM SIGGRAPH Course Notes, August 2007. Award: Best Course Notes for a New Course.

[4] Henrik Wann Jensen. Global illumination using photon maps. In *Proceedings of the Eurographics Workshop on Rendering Techniques '96*, pages 21–30, London, UK, UK, 1996. Springer-Verlag.

[5] J. T. Kajiya and T. L. Kay. Rendering fur with three dimensional textures. *SIGGRAPH Comput. Graph.*, 23(3):271–280, July 1989.

[6] Stephen R. Marschner, Henrik Wann Jensen, Mike Cammarano, Steve Worley, and Pat Hanrahan. Light scattering from human hair fibers. *ACM Trans. Graph.*, 22(3):780–791, July 2003.

[7] Jonathan T. Moon and Stephen R. Marschner. Simulating multiple scattering in hair using a photon mapping approach. *ACM Trans. Graph.*, 25(3):1067–1074, July 2006.

[8] Kelly Ward, Florence Bertails, Tae yong Kim, Stephen R. Marschner, Marie paule Cani, and Ming C. Lin. A survey on hair modeling: styling, simulation, and rendering. In *IEEE TRANSACTION ON VISUALIZATION AND COMPUTER GRAPHICS*, pages 213–234, 2006.

[9] Arno Zinke, Cem Yuksel, Andreas Weber, and John Keyser. Dual scattering approximation for fast multiple scattering in hair. *ACM Trans. Graph.*, 27(3):32:1–32:10, August 2008.